

## First Solar energetic particles measured on the Lunar far-side

ZIGONG XU <sup>1</sup>, JINGNAN GUO <sup>2,3,1</sup>, ROBERT F. WIMMER-SCHWEINGRUBER <sup>1</sup>, JOHAN L. FREIHERR VON FORSTNER <sup>1</sup>,  
HENNING LOHF<sup>1</sup>, YUMING WANG<sup>2,3</sup>, NINA DRESING <sup>1</sup>, SHENYI ZHANG<sup>4,5,6</sup>, BERND HEBER<sup>1</sup> AND MEI YANG<sup>7</sup>

<sup>1</sup>*Christian-Albrechts-Universität zu Kiel*

*Institut für Experimentelle und Angewandte Physik*

<sup>2</sup>*CAS Key Laboratory of Geospace Environment, University of Science and Technology of China, Hefei 230026, China*

<sup>3</sup>*CAS Center for Excellence in Comparative Planetology, Hefei 230026, China*

<sup>4</sup>*National Space Science Center, Chinese Academy of Sciences, Beijing, China*

<sup>5</sup>*Beijing Key Laboratory of Space Environment Exploration, Beijing, China*

<sup>6</sup>*University of Chinese Academy of Science, Beijing, China*

<sup>7</sup>*Beijing Institute of Spacecraft System Engineering, Beijing, China*

(Received \* \* , 2020; Revised \* \* , 2020; Accepted December 22, 2024)

Submitted to ApJ L

### ABSTRACT

On 2019 May 6, the Lunar Lander Neutron & Dosimetry (LND) Experiment on board the Chang'E-4 on the far-side of the Moon detected its first small solar energetic particle (SEP) event with proton energies up to 21MeV. Combined proton energy spectra are studied based on the LND, *SOHO*/EPHIN and *ACE*/EPAM measurements which show that LND could provide a complementary dataset from a special location on the Moon, contributing to our existing observations and understanding of space environment. Velocity dispersion analysis (VDA) has been applied to the impulsive electron event and weak proton enhancement and the results demonstrate that electrons are released only 22 minutes after the flare onset and  $\sim 15$  minutes after type II radio burst, while protons are released more than one hour after the electron release. The impulsive enhancement of the in-situ electrons and the derived early release time indicate a good magnetic connection between the source and Earth. However, stereoscopic remote-sensing observations from Earth and STA suggest that the SEPs are associated with an active region nearly  $100^\circ$  away from the magnetic footpoint of Earth. This suggests that the propagation of these SEPs could not follow a nominal Parker spiral under the ballistic mapping model and the release and propagation mechanism of electrons and protons are likely to differ significantly during this event.

*Keywords:* Solar energetic particles, Space Radiation, Lunar Exploration

### 1. INTRODUCTION

The Chang'E-4 mission, which consists of a lander, a rover and a relay satellite, is humanity's first mission landing on the lunar far-side, located at von Kármán Crater. The Lunar Lander Neutron and Dosimetry experiment (LND) (Wimmer-Schweingruber et al. 2020) on board the lander of Chang'E-4 is designed to take active dosimetry measurements on the surface of the Moon as its chief scientific goal. Apart from the primary objective of LND which is to measure the radiation level on the lunar far-side preparing for astronaut missions (Zhang et al. Science advance, accepted), the charged particle telescope could also provide high quality data of energetic particles and contribute to heliophysics. For example, LND can provide protons and Helium-4 spectra between 9 MeV/nuc and 35 MeV/nuc.

However, during the first mission year (2019), due to the solar minimum activity, LND detected only one SEP event on May 6, 2019 with a significant statistic for protons ranging between 9.0 and 21.0 MeV<sup>1</sup>. This event was related

Corresponding author: Zigong, Xu., Jingnan, Guo  
xu@physik.uni-kiel.de, jnguo@ustc.edu.cn

<sup>1</sup> We note that a small enhancement of energetic particles above the nominal GCR background is visible between May 4 and May 6 as in Fig.2. But due to its low statistics, we cannot confirm it being an SEP event.

**Table 1.** Time line of the SEP event on 6 May 2019

Time(UT)	Event	Character	Refer to
2019.05.06			
04:56:00	Eruption of Flare and start of SXR	AR 12740@50°E; M1.0 class $D_E = 101^\circ$ ; $D_{STA} = 7^\circ$	
04:57:23	Type III radio burst	SSRT,WIND/WAVES,STA/SWAVES	
05:00:22	EUV wave propagating toward west	AIA 193Å; $V \approx 500\text{km/s}$	Fig. 1
05:03:30	Type II radio burst	@230MHz – 90MHz, Last for 6 minutes	
05:18:24	Electron release	VDA, IMF~1.18AU, beam-like	Fig. 3
05:28:00	CME first appears at SOHO/LASCO C2	376km/s <sup>a</sup> ;326km/s <sup>b</sup>	Appendix
05:30:59	310keV electron onset	WIND	Fig.3
05:31:00	CME at STA COR2	AW~20°, deflect to west	
06:27:00	10.7-12.7MeV proton release	LND;TSA	
06:29:42	Proton release	VDA, IMF~1.36AU	Fig. 3
07:32:00	10.7-12.7MeV proton onset	LND, Poisson-CUSUM (Lucas 1985)	Appendix

NOTE—All the time in this table has already considered the  $\sim 8.3$  minutes light travel time;  $D_E$  is the longitudinal distance between active region and magnetic footpoint of the Earth;  $D_{STA}$  is the distance to the STA footpoint; SSRT = Siberian Solar Radio Telescope; AW = angular width; GOES = Geostationary Operational Environmental Satellite; VDA = velocity dispersion analysis; IMF = interplanetary magnetic field; TSA = Time shifted analysis

<sup>a</sup> Velocity from Cactus catalog

<sup>b</sup> Velocity from GCS fitting

to an active region located at E50, nearly 100° away from the Earth’s nominal coronal magnetic footpoint, where an M1.0 class flare erupted before the SEPs onset and a narrow and slow coronal mass ejection (CME) appeared later. Combining remote sensing observations of the solar source with in-situ particle measurements from multiple spacecraft, we analyze and discuss about the possible particle release and transport processes in the interplanetary space.

## 2. OBSERVATIONS

### 2.1. Remote-sensing observations

On 2019 May 6, an M1.0 class flare erupted from active region (AR) 12470 located at N08E50. The soft X-ray (SXR) flare had an onset at 04:56:00<sup>2</sup> and lasted for  $\sim 8$  minutes as detected by the solar X-ray Imager (SXI) on the GOES satellite. Since this is the only visible eruptive source on the Sun seen from Earth before the onset of the SEPs, we believe this is the solar counterpart of the SEPs measured in situ near Earth and Moon. Nearly at the same time of the SXR emission, a broadband type III radio burst starting from 240 MHz was observed by not only the ground radio observatory Solar Radio Telescope (SSRT<sup>3</sup>) on Earth but also by the WAVES instrument on board the WIND spacecraft at Earth L1 point as well as by WAVES on board STEREO-A (STA). A type II radio burst between 230–90 MHz indicating the existence of a coronal shock has been then reported by the SSRT during 05:03:30–05:09:30. The timeline of this event is given in Tab.1.

At 05:00:20, an asymmetric EUV wave started propagating toward the north-western hemisphere from the source as observed in the 193Å band of the Atmospheric Imaging Assembly (AIA) on board the Solar Dynamics Observatory (SDO). The outer edges of the wave front at different times, i.e, at 05:00, 05:02, 05:07, 05:12, 05:17, 05:22 on May 6, are marked as colored dashed lines in Fig.1 which is explained in more details below. After 05:22, the wave continued expanding at the solar surface with a rather faint structure which does not contain a clear wave front.

About half an hour after the flare eruption, at 05:28, a CME first appeared in the field of view of the Large Angle and Spectrometric Coronagraph Experiment (LASCO) C2 of the *Solar and Heliospheric Observatory* (SOHO) with a projected speed of 376 km/s and an angular width of 20°, as reported in the CACTUS CME catalog<sup>4</sup>. Simultaneously, STA COR2 also captured the same structure. We applied the Graduated Cylindrical Shell (GCS) Model (Thernisien

<sup>2</sup> The time for remote-sensing measurements in this study has subtracted the  $\sim 8.3$  minutes light travel time over 1 AU distance.

<sup>3</sup> <http://www.e-callisto.org/>

<sup>4</sup> <http://sidc.oma.be/cactus/>

2011) to the Coronagraph observations from two directions to obtain the velocity and propagation direction of the CME. In the bottom panel of Fig.1, we give the CME observation and outlines the fitted CME structure in green at 05:46 on May 6. The fitting results show that the linear speed of the CME front was about 326 km/s and the CME was deflected by about 10 degrees away from the location of the flare to the west, consistent with the direction of the EUV wave propagation.

In Fig.1, the magnetic field lines reconstructed using the potential field source-surface (PFSS) model is shown as an overlay on the magnetogram map of Carrington rotation 2217 from the Global Oscillation Network Group (GONG, <https://gong.nso.edu>). Open magnetic field lines with positive polarity shown in green and negative polarity shown in red are generally considered as the main channels for SEP propagation. The polarity inversion line is shown in blue. The above mentioned active region AR12470 is on the right part of the plot marked by the white arrow. The radial projection points of STA and Earth on the solar surface on May 6 are plotted as open circles in black and blue, respectively. The magnetic footpoints based on the ballistic mapping of the solar wind propagating at an average solar wind speed (about 440 km/s as observed in situ at Earth) are marked as filled circles. We note that the magnetic footpoint of STA is only  $7^\circ$  away from the location of AR12470, which suggests STA is well connected to this active region. On the other hand, the longitudinal separation between the flare and Earth's footpoint is about  $100^\circ$  as displayed in Fig. 1.

## 2.2. In-situ measurements

LND is the first-ever instrument on the lunar far-side that measures the Lunar surface radiation environment and charged particles. By recording the energy deposition of a particle through a set of 10 detectors, LND can stop and thus identify the species and energy of charged particles up to 30 MeV/nuc. In order to better understand the temporal variation of protons and electrons at other energies during the event, we also include observations from the Electron Proton Helium Instrument (EPHIN, Müller-Mellin et al. 1995) on board SOHO, the Electron Proton Alpha Monitor (EPAM, Gold et al. 1998) on board the Advanced Composition Explorer (ACE), as well as 3-D Plasma and Energetic Particle Investigation (3DP, Lin et al. 1995) on board WIND.

After the flare eruption at 04:56 on May 6 which is marked as a red vertical dashed line in Fig.2, LND detected the arrival of SEPs as shown in panel (a) of Fig.2. The proton channel 9.0-21.0MeV shown here is the combination of the first five channels of LND's one-minute proton data which are provided in appendix. Due to the low intensity of the event and poor statistics in the data, the flux is averaged for each 30 minutes. However, for this event there are some data gaps in the EPHIN measurement due to SOHO just finishing a roll maneuver on May 6 accounting for the antenna issue of the spacecraft resulting in limited telemetry, as shown in panel (b) which displays the 4.3–7.8 MeV proton intensity profile. Thus, LND becomes the only instrument that observed the complete duration of this event at these energies.

Both y-axes in panels (a) and (b) are plotted in linear scale in order to better show the SEP enhancement. Panel (c) shows the ion flux averaged over each 30 minutes for two energy channels between 1 and 4.75 MeV detected by the LEMS30 (Low-Energy Magnetic Spectrometer) detector, one telescope aperture of ACE/EPAM. The intensity profile shows a clear velocity dispersion of ions which are mostly attributed to protons.

Finally the electron profile observed by WIND between 40 keV and 180 keV is plotted in panel (d) which clearly shows electrons starting to arrive at around 5:30 on May 6, slightly earlier than the energetic protons. Different energy channels show different onset times with higher energy electrons arriving earlier and this velocity dispersion feature is studied using a velocity dispersion analysis (VDA) method as discussed below. The second increase later that day is associated to another solar eruption which is not considered in this study.

It should also be noted that between May 4 and May 6, another group of energetic particle events are registered by all four instruments. However, the proton intensity in LND is too weak to determine the onset time and SOHO/EPHIN contains a large data gap. This event is therefore not studied here.

The remaining panels of Fig. 2 show the local solar wind plasma data measured by ACE including the magnetic field, solar wind speed, proton density. Upon the onset of the SEP event, the near-Earth space is rather calm with no indication of transient Interplanetary coronal mass ejections (ICMEs), shocks or stream interaction regions(SIR) which could otherwise contribute to possible local acceleration of particles. However, a few days earlier on May 3 and May 4, there was an SIR structure suggested by the increase of magnetic fields, compressed proton density and delayed enhancement of plasma velocity as highlighted in the red area.

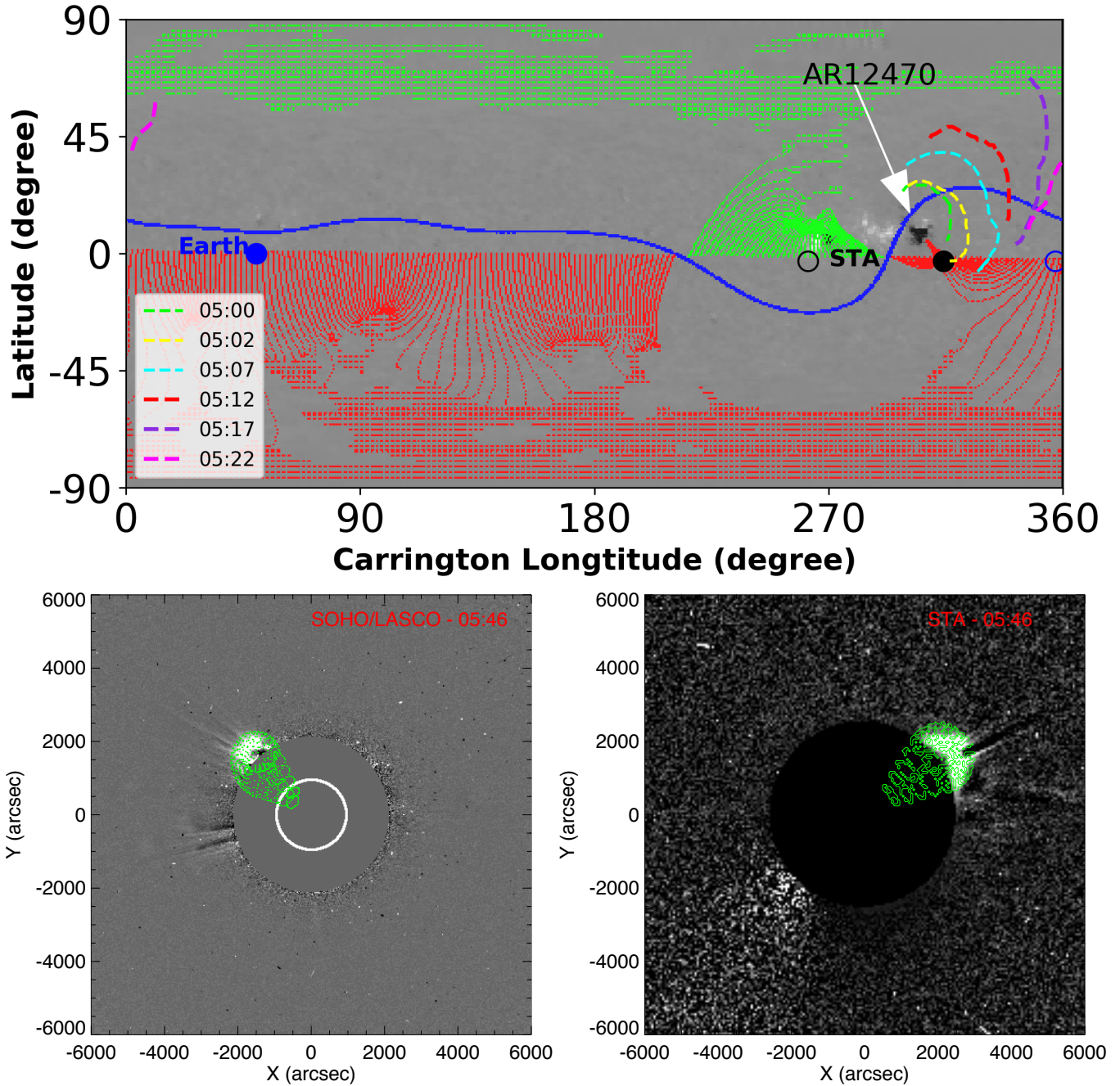


**Figure 1.** Top: The synoptic ecliptic-plane field plot for the Carrington rotation 2217. The projected locations of STEREO-A (STA) and Earth are added as open circles and their magnetic footpoints mapped back at 2.5 solar radii based on the ballistic model are shown as filled circles. The outer edges of an EUV wave front at different times, i.e., at 05:00, 05:02, 05:07, 05:12, 05:17, 05:22 on May 6, are marked as colorful dashed lines. Bottom: CME observation of SOHO/Lasco (left) and STA/Cor2 (right) at 05:46 on May 6, 2019. The green mesh outlines the graduated cylindrical shell (GCS) reconstruction of the CME geometry.

As shown in the bottom of Fig. 2, at the time of the SEP event under study, the longitudinal separation between the active region and the magnetic footpoint of STA using ballistic back mapping is only  $7^\circ$  which suggests that STA would be a perfect observer for these energetic particles. However, the SEP was not detectable due to a strong ion/proton event, ICME and IP shock passage from a previous event occurring on May 4 while the electron channel were strongly contaminating by these ions.

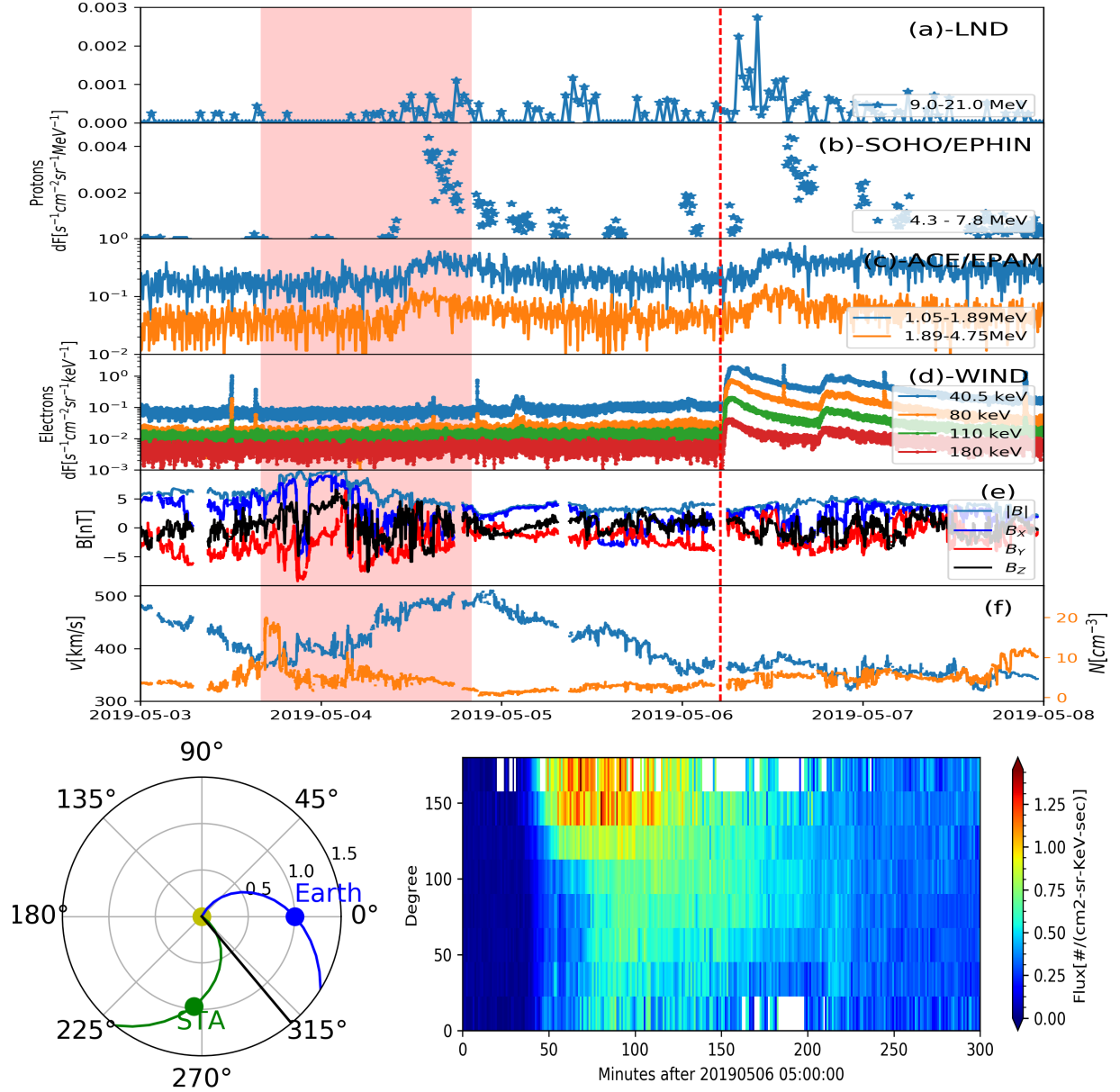


**Figure 2.** In-situ measurements near Earth, including (a) proton flux in 9.0-21.0 MeV by *LND*, (b) proton flux in 4.3-7.8 MeV by *SOHO/EPHIN*, (c) ion flux in 1.05-4.75 MeV by LEMS120 of *ACE/EPAM*, (d) electron flux in 40.5 keV-180 keV by *WIND/3DP*, (e) magnetic field magnitude and three components in the GSE coordinates, (f): solar wind velocity and plasma density. The red line indicates the eruption time of solar flare on May 6. The radial direction of the active region as well as the nominal Parker spirals for Earth and STA are plotted in the HEEQ coordinate in the bottom left panel. The pitch angle distribution of electrons in 50-80 keV measured by *WIND/3DP* after 05:00:00 on May 6 are given in bottom right panel. Red highlighted areas are stream interaction regions(SIR) passing the Earth several days before the SEP event.

### 2.3. Determination of onset and release times

The small SEP event intensity along with the small geometry factor of *LND* require at least a half-hour averaging of the intensity data and therefore significantly limit the determination of the event onset times. Therefore, we apply the Poisson-CUSUM method (Lucas 1985) and follow the procedure in (Huttunen-Heikinmaa et al. 2005) to derive the onset time of each energy channel. In appendix, we show the Poisson-CUSUM analysis on the different *LND* energy channels.

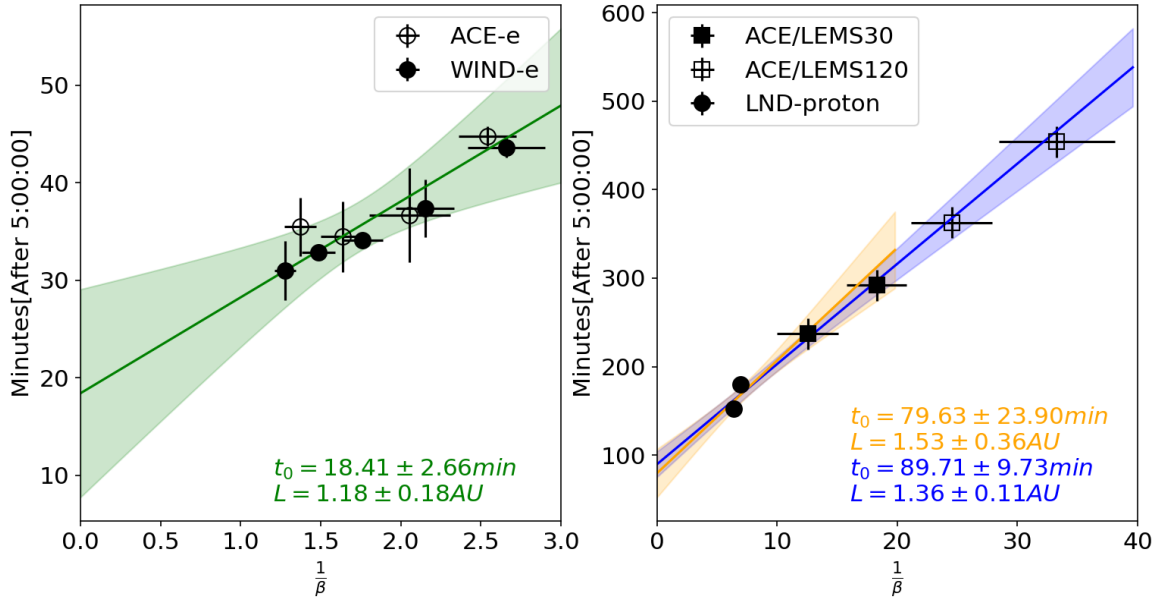


**Figure 3.** Velocity dispersion analysis of the SEPs (electrons shown in the left and protons shown on the right panel) on May 6, 2019. *WIND* and *ACE* electron data are used to determine the electron release time. LND proton, *ACE/EPAM* LEMS30 and LEMS120 ion data are used to determine the proton release time. The linear fits and the fitted parameters of the VDA analysis with 95% confidence interval are marked in the plots. More details can be found in the text of Sec. 2.3.

The onset times of the 9.0–10.6 MeV and 10.7–12.7 MeV channels are 08:00 and 07:32, respectively, based on 1-minute data products. Assuming protons travelling scatter-free along a 1.2 AU interplanetary magnetic field (IMF) line, which is calculated from the solar wind speed averaged over three days before the SEP event, we derive that the 10.7–12.7 MeV protons need about 63 minutes to arrive at Earth and the release time is around  $06:29 \pm 1$  min. As for other data from *ACE/EPAM* and *WIND/3DP*, the onset times are determined as the flux exceeds  $3\sigma$  of the background signal which is defined as the flux an hour before the SEP onset.

In Fig. 3, the onset times  $t_{onset}$  of different channels are plotted versus  $1/\beta$  that is  $c/v$ , where  $c$  is the speed of light and  $v$  is the speed of particles with different energies. The uncertainty of the onset time is assumed as the difference between  $1\sigma$  and  $3\sigma$  level. The error bar in the x direction is the bin width of the energy channels. Both *ACE/EPAM* and *WIND/3DP* onset times of electrons are plotted in the left panel of Fig.3. Proton onset times are plotted in the right panel with the *ACE/EPAM* LEMS30 channels shown in filled square, LEMS120 in empty square and high-energy LND channels shown in filled circle. Since only two channels of LEMS30 are available, another two channels from LEMS120 with lower energy are also referred here.

Given the determined onset time at different energy channels, the VDA method can be applied to derive the particle release time. Considering the uncertainties in both x and y directions in Fig. 3, we fit the data with a function  $t_{onset} = t_0 + L/v$  using the orthogonal distance regression (ODR) method. Here,  $t_{onset}$  and  $v$  are readily known with  $t_0$  and  $L$  to be fitted.  $t_0$  is the particle release time and  $L$  is the IMF line along which particles propagate from the Sun to Earth assuming that all particles with different energies propagate along the same path. This condition is more likely met when no cross-field scattering or diffusion are considered. As discussed before,  $L$  is typically 1.2 AU given a 400 km/s solar wind speed under undisturbed IMF conditions. The linear fits of VDA are plotted as solid lines in the left and right panels of Fig. 3 for electrons and protons, respectively and 95% confidence intervals are given in shadows. Fitting result based on protons from the LND and LEMS30 measurements is given in orange, while the fit using all data is plotted in blue. The results of  $t_0$  and  $L$  are also given in Tab.1 and as legends in the plots. It is shown that the fits from two groups of data are consistent within the error bar.

Their values suggest that electrons are released  $22.41 \pm 2.66$  minutes after the flare eruption and that protons are released about  $71.3 \pm 12.39$  minutes after the electron release. The IMF lengths for the electron propagation is about

$1.18 \pm 0.18$  AU which is consistent with the Parker spiral derived from the in-situ solar wind speed. However, the derived  $L$  for protons is longer, i.e,  $1.36 \pm 0.11$  AU, suggesting that the interplanetary transport of protons may be quite different from electrons despite that they result from the same event.

The VDA method assumes that all particles stream along the same IMF which may become invalid in a realistic condition. In order to assess the reliability of this assumption for this SEP event, we also checked the pitch-angle measurement by *WIND*. At the beginning of the SEP event, electrons show a clear anisotropy (enhanced intensity at  $\sim 180^\circ$  pitch angle, bottom right panels of Fig.2) suggesting that electrons first arrived along the IMF (Tab.1). Consequently, these particles experienced little scattering, in agreement with the requirement of the VDA method. Unfortunately, proton observations with much smaller statistics make it difficult to identify a significant anisotropy of protons from *WIND*. Therefore, we cannot be sure if protons propagated along the same IMF as electrons or if they suffered different propagation conditions.

#### 2.4. Energy Spectra

Combining the proton measurement by *SOHO*/EPHIN as shown in panel (b) of Fig. 2 and the ions registered by *ACE*/EPAM in panel (c) which are dominated by lower energy protons and also those of LND, we plot the proton spectra integrated between 06:00 and 17:00 on May 6, 2019 in the left panel of Fig.4. The areas shaded in blue, green, and pink are the energy coverage of LND (9 MeV–35 MeV), *SOHO*/EPHIN (4.3 MeV–7.8 MeV) and *ACE*/EPAM (0.310 MeV–4.75 MeV) respectively. The background GCR spectra are also plotted and they are averaged between April 29 and May 3 (LND started working on April 29 for its fifth lunar day measurement). The energetic proton spectra during the event are well above the background as shown in the left panel, despite of the large uncertainty in the LND data due to the low number of counts. The right panel of the figure shows the SEP spectra with background spectra subtracted. Because of the EPHIN data gap during the impulsive phase of the SEP event as shown in Fig. 2, the actual spectral flux of the SEPs should be larger than the derived one, as pointed out by a green arrow in the right panel.

We use a classical double power-law spectrum to fit the data, and the power-law indices are  $-0.93 \pm 0.18$  and  $-3.13 \pm 0.38$  for the spectra below and above the broken energy, respectively. Unlike other large SEP events whose broken energy is normally above 10 MeV (Mewaldt et al. 2012), this event has a lower broken energy at around 2.5 MeV which is the intersection point of the two power law spectra.

### 3. SUMMARY AND DISCUSSION

On 2019 May 6, a small SEP event was observed by LND at the far-side of the Moon. Despite of its low intensity and low radiation risk, this is the first SEP event ever detected on the surface of the Moon. This event was also detected by *SOHO*/EPHIN, which unfortunately only registered its decay phase. The only possible solar source associated is a flare and its accompanying CME at AR 12470 located on the east hemisphere. The type II radio burst indicates the existence of a shock driven by the CME despite of its low velocity,  $\sim 326$ km/s as fitted by the GCS model.

The time profiles of electrons and protons clearly show velocity dispersion. According to the VDA analysis which assumes that all particles propagate along the same IMF line arriving at Earth, electrons were released about  $22.41 \pm 2.66$  minutes after the flare and type III radio burst and about 8 minutes after the high frequency type II radio burst, while protons were released at least 70 minutes later. The in-situ velocity dispersion and anisotropy of electrons suggest that a direct magnetic connection from the source to Earth was established for these electrons. However, the separation between the flare location and the magnetic footpoint of Earth derived from the standard ballistic mapping is as large as  $101^\circ$ . Alternatively, the magnetic footpoint of STA is only about  $7^\circ$  away from the flare and STA's observation cannot confirm particle enhancement associated with this eruption. This is a very surprising result considering the classical scenario of particle transport during small impulsive events (Reames 1999): accelerated particles stream along an open IMF connecting the source and the observer with high-energy ones arriving earlier than lower energy ones. While the in-situ electron observation of this event at Earth (impulsive, velocity dispersion, beam-like distribution) supports this picture, the remote sensing observation contradicts this explanation. Unfortunately, there is no observation of iron charge states which could give more information of the acceleration source.

One possible scenario could be that particles are accelerated by the shock deviated westwards reaching the magnetic footpoint of Earth, as indicated by the westward propagating EUV waves seen by SDO (Fig. 1). For example, Rouillard et al. (2012) have found the association between EUV waves and particle release in large separated SEPs. The GCS fitting of the CME also indicates a non-radial and westward-deflected propagation towards the location of the Earth

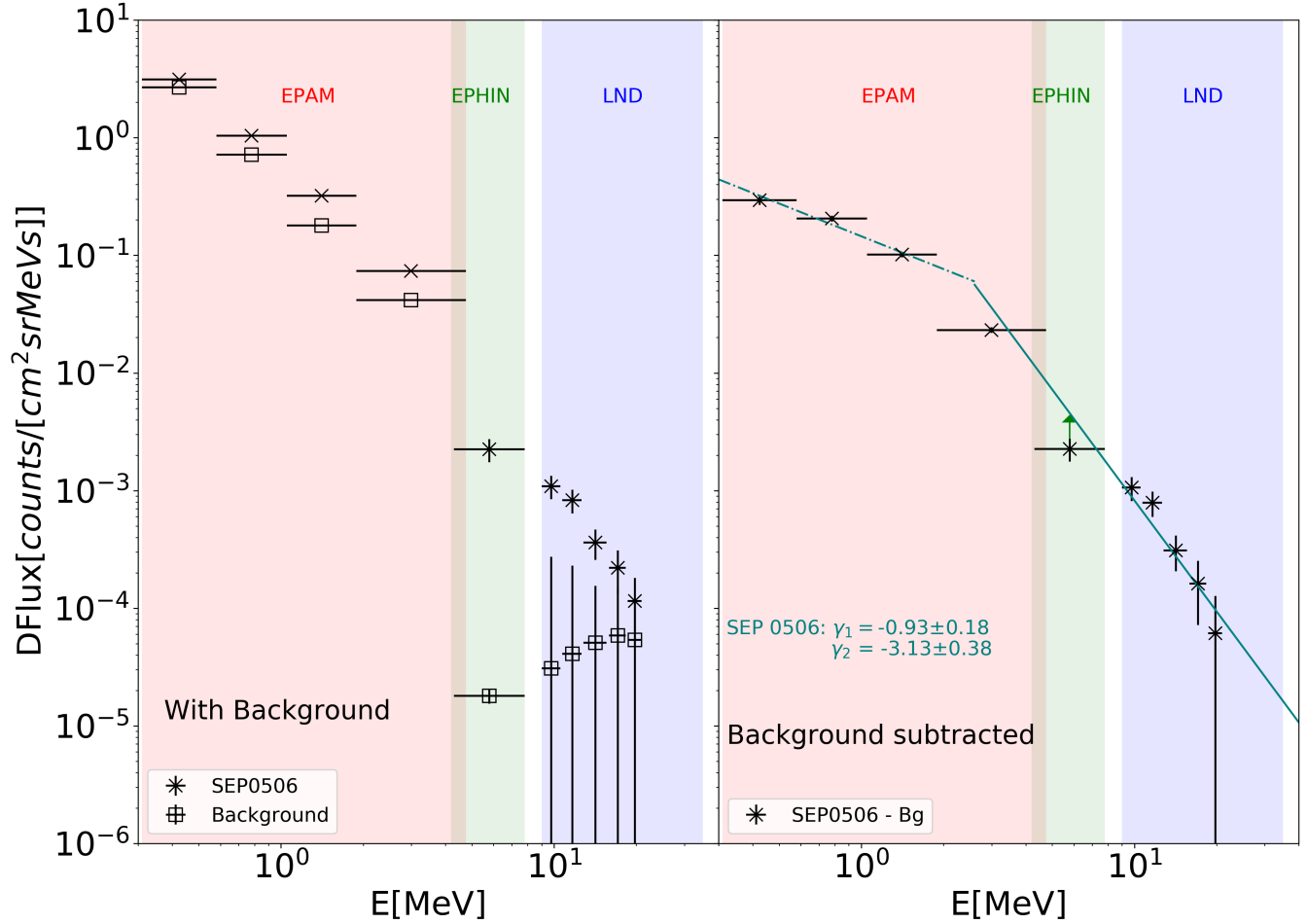


**Figure 4.** Proton spectra of the SEPs on May 6, 2019 and the background spectra which are averaged between April 29 and May 3. The left panel shows the spectra including the background and the right panel shows the SEP spectra with background subtracted. Different shaded areas indicate the energy ranges covered by the different instruments from  $\sim 300$  keV to  $\sim 30$  MeV. More details can be found in the text of Sec. 2.4.

footpoint. However, the deflection is only about  $10^\circ$  and the EUV wave became rather faint after 05:25 suggesting the shock was unlikely to reach Earth’s footpoint upon the particle release time. Therefore, it is difficult to conclude that a deviated shock could be fully responsible for the initial particle acceleration and release processes.

The in-situ electrons observed at Earth suggest a good magnetic connection to the release location at the Sun, which is, however, inconsistent with the remote-sensing observations and the standard Parker spiral model. Therefore, the magnetic field configuration based on the simple PFSS and Parker spiral model might be inaccurate to explain the SEP transport during this event.

Klassen et al. (2018) showed an example of electrons accelerated by flares reaching a very distant magnetic footpoint ( $90^\circ$ ) of STA through an irregular magnetic field at the solar source. The PFSS extrapolation of the magnetic field before this eruption does not show any direct connection between the flare and the location of Earth’s footpoint. As PFSS model, assuming a current-free field by definition, is an idealised consideration of the solar corona, the real magnetic configuration during solar activities might be drastically different. Besides, solar eruptions often rearrange the solar magnetic fields through e.g., magnetic re-connection, and a possible path might have existed for particles to propagate across such a big heliospheric longitudinal distance. Unfortunately, there is no sufficient remote-sensing observation to conclude this scenario.

Moreover, the Parker spiral model is also an over-simplified non-disturbed IMF condition and some researchers suggest the meandering and “random walk” of IMF would affect the particle propagation in the heliosphere (e.g., Mazur et al. 2000; Laitinen et al. 2016). Besides, the cross-field transport due to pitch angle scattering and diffusion

process might also cause particles to propagate across field lines to be observed far away from the center of the solar eruption (e.g., [Wibberenz & Cane 2006](#)).

Another intriguing fact about this event is the long delay between the electron and proton release times as derived from the VDA model which indicates that different acceleration processes and/or release locations might be responsible for protons and electrons. As protons are released much later, they may be more likely accelerated by the shock which, however, can not be confirmed to have reached Earth's magnetic footpoint. [Richardson et al. \(2014\)](#) have carried out a thorough study of the delay times for the in-situ proton/electron events with respect to their solar sources. They found some statistical and empirical correlations of the onset time delay versus the longitudinal separation of the footpoint and the flare. The electron and proton delay times of our event actually are within the uncertainties of their functions.

It is worth noting that an ICME driven shock arrived at STA later on May 6 which was traveling en-route towards STA upon the SEP event. This ICME might have disturbed the IMF condition distorting the normal Parker spirals (e.g., [Lario et al. 2020](#)) along which particles are most efficiently transported and led to the absence of SEPs (or not statistically significant) detected by STA. Besides, the ICME-driven shock may form discontinuity boundaries that make it difficult for particles to transverse across ([Strauss et al. 2016](#); [Guo et al. 2018](#)).

To summarize, we have presented various observational facts of the first SEP event ever observed on the Lunar surface. Despite of its weak intensity and insignificant heliospheric impact, this event is rather intriguing and cannot be easily explained by the classical impulsive event features which require a good magnetic connection between the observer and the solar source. We believe more stereoscopic and simultaneous in-situ and remote-sensing observations would be beneficial for a thorough analysis of such events. We also highlight the importance of developing theories and models which are more complex and realistic than simple PFSS and Parker spiral models for better understanding the particle transport in the heliosphere.

#### ACKNOWLEDGMENTS

The Lunar Lander Neutron and Dosimetry (LND) instrument is supported by the German Space Agency, DLR, and its Space Administration under grant 50 JR 1604 to the Christian-Albrechts- University (CAU) Kiel and supported by Beijing Municipal Science and Technology Commission, Grant No. Z181100002918003 and National Natural Science Foundation of China Grant: 41941001 to the National Space Science Center (NSSC). The scientific data are provided by China National Space Administration. J. Guo and Y. Wang are supported by the Strategic Priority Program of the Chinese Academy of Sciences (Grant No. XDB41000000 and XDA15017300), and the CNSA pre-research Project on Civil Aerospace Technologies (Grant No. D020104). N.D. was supported under grant 50OC1302 by the Federal Ministry of Economics and Technology on the basis of a decision by the German Bundestag. I also would like to express my very great appreciation to Patrick Kühl and Andreas Klassen for their valuable suggestions on this work.

#### REFERENCES

- Gold, R. E., Krimigis, S. M., Hawkins, III, S. E., et al. 1998, *SSRv*, 86, 541, doi: [10.1023/A:1005088115759](https://doi.org/10.1023/A:1005088115759)
- Guo, J., Dumbović, M., Wimmer-Schweingruber, R. F., et al. 2018, *Space Weather*, 16, 11561169
- Huttunen-Heikinmaa, K., Valtonen, E., & Laitinen, T. 2005, *A&A*, 442, 673, doi: [10.1051/0004-6361:20042620](https://doi.org/10.1051/0004-6361:20042620)
- Klassen, A., Dresing, N., Gómez-Herrero, R., Heber, B., & Veronig, A. 2018, *A&A*, 614, A61, doi: [10.1051/0004-6361/201732041](https://doi.org/10.1051/0004-6361/201732041)
- Laitinen, T., Kopp, A., Effenberger, F., Dalla, S., & Marsh, M. S. 2016, *A&A*, 591, A18, doi: [10.1051/0004-6361/201527801](https://doi.org/10.1051/0004-6361/201527801)
- Lario, D., Kwon, R. Y., Balmaceda, L., et al. 2020, *ApJ*, 889, 92, doi: [10.3847/1538-4357/ab64e1](https://doi.org/10.3847/1538-4357/ab64e1)
- Lin, R., Anderson, K., Ashford, S., et al. 1995, *Space Science Reviews*, 71, 125
- Lucas, J. M. 1985, *Technometrics*, 27, 129, doi: [10.1080/00401706.1985.10488030](https://doi.org/10.1080/00401706.1985.10488030)
- Mazur, J. E., Mason, G. M., Dwyer, J. R., et al. 2000, *ApJL*, 532, L79, doi: [10.1086/312561](https://doi.org/10.1086/312561)
- Mewaldt, R.,Looper, M., Cohen, C., et al. 2012, *Space Science Reviews*, 171, 97
- Müller-Mellin, R., Kunow, H., Fleißner, V., et al. 1995, *Solar Physics*, 162, 483
- Reames, D. V. 1999, *SSRv*, 90, 413, doi: [10.1023/A:1005105831781](https://doi.org/10.1023/A:1005105831781)
- Richardson, I. G., von Rosenvinge, T. T., Cane, H. V., et al. 2014, *SoPh*, 289, 3059, doi: [10.1007/s11207-014-0524-8](https://doi.org/10.1007/s11207-014-0524-8)

- Rouillard, A. P., Sheeley, N. R., Tylka, A., et al. 2012, ApJ, 752, 44, doi: [10.1088/0004-637X/752/1/44](https://doi.org/10.1088/0004-637X/752/1/44)
- Strauss, R. D., le Roux, J. A., Engelbrecht, N. E., Ruffolo, D., & Dunzlaff, P. 2016, ApJ, 825, 43, doi: [10.3847/0004-637X/825/1/43](https://doi.org/10.3847/0004-637X/825/1/43)
- Thernisien, A. 2011, ApJS, 194, 33, doi: [10.1088/0067-0049/194/2/33](https://doi.org/10.1088/0067-0049/194/2/33)
- Wibberenz, G., & Cane, H. V. 2006, ApJ, 650, 1199, doi: [10.1086/506598](https://doi.org/10.1086/506598)
- Wimmer-Schweingruber, R. F., Yu, J., Böttcher, S. I., et al. 2020, arXiv e-prints, arXiv:2001.11028. <https://arxiv.org/abs/2001.11028>

## APPENDIX

## A. LND MEASUREMENT AND POISSON-CUSUM ANALYSIS

The charge particle telescope of LND could measure protons in one-minute time resolution between 9.0–35 MeV and the explicit energy bins are given in Table. 6 of [Wimmer-Schweingruber et al. \(2020\)](#). Here, we present the proton count rates in 9.0–10.6 MeV, 10.7–12.7 MeV and 12.8–15.7 MeV during May 4 and May 8 in Fig.5 and use the same time resolution (30 minutes) as the panel(a) of Fig.2. Those blue curve indicate a bad statistic for those channels. For example, the peak count number the LND registered every half an hour in 9.0–10.6 MeV is only 5. Therefore, the profile could not be able to determined the onset time directly, especially the channels above 15.7MeV which are not shown here.

In order to calculate the event onset time precisely, the Poisson-CUSUM method are applied here and the results are plotted in a orange line for each channel. Cumulative sum (CUSUM) control schemes are widely used in industrial applications for detecting small shift. By the definition of control schemes, the difference between the observed value  $Y_i$  and a reference value  $k$  are accumulated as a systematic change which is:

$$S_i = \max(0, Y_i - k + S_{i-1}) \quad (\text{A1})$$

The start values is  $S_0 = 0$  in standard CUSUM.

The reference value  $k$  is determined below:

$$k = \frac{\mu_d - \mu_a}{\ln(\mu_d) - \ln(\mu_a)} \quad (\text{A2})$$

where  $\mu_a$  is the mean number of counts estimated for each channel during the pre-event background and  $\mu_d$  is selected by a two-sigma-shift criterion([Huttunen-Heikinmaa et al. 2005](#)):

$$\mu_d = \mu_a + 2\sigma_a \quad (\text{A3})$$

$\sigma_a$  is the standard deviation of the pre-event background.

When the systematic change exceed the decision values  $h$ , then the onset of the SEP event are determined. Here we give a small decision values  $h = 1$  according to the table in [Lucas \(1985\)](#). In order to reduce the false alarm due to the small  $h$ , we need to check the following 29 data points after the presumed onset before. If all of them are larger than  $h$ , then the first signal is the onset time of SEP event.

We then apply the Poisson-CUSUM method for the one-minute data and the systematic changes are plotted as orange line in Fig. 5. The red dashed vertical line marks the eruption time of flare at 04:46 on May 6. After that, the systematic changes raised more clearly than the origin data and last for a long time. The first data points of three channel during May 6 that are larger than 1 now is easy to be determined. Obviously, in our case that signals are also the onset time of the SEPs. The onset time of the 9.0–10.6 MeV and 10.7–12.7 MeV channels are 08:00 and 07:32 respectively and for 12.8–15.7 MeV, the onset time is around 09:30. The third channel has larger uncertainty due to the low statistic, i.e., 2 counts/30 minutes at the peak, and is not considered when determine the particle release time. Another two channels above 15.7MeV have even worse statistic and the Poission-CUSUM method is inapplicable.

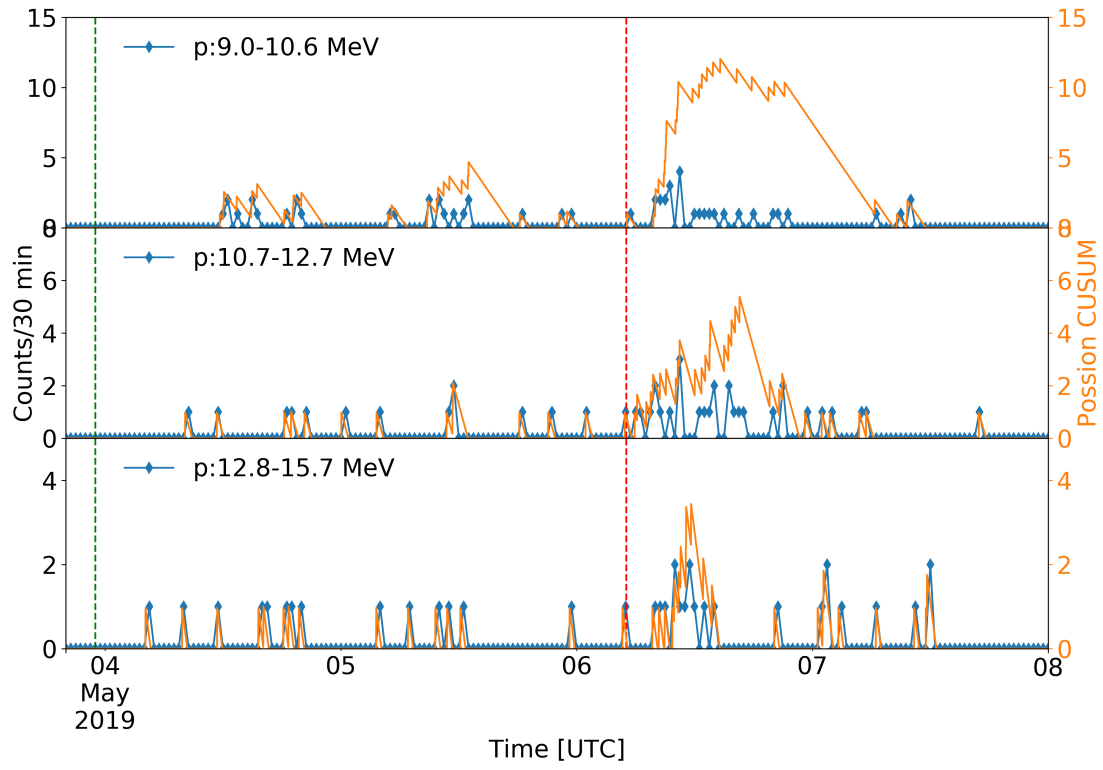


**Figure 5.** LND proton count rate in half an hour cadency(blue) and Poisson-CUSUM analysis(orange) based on one-minute data.